The Astrophysical Journal Letters, 854:L32 (4pp), 2018 February 20 https://doi.org/10.3847/2041-8213/aaad5e

The Redshift of the BL Lac Object TXS 0506+056

Simona Paiano[1,2], Renato Falomo[1], Aldo Treves[3,4], and Riccardo Scarpa[5,6]
[1] INAF, Osservatorio Astronomico di Padova, Vicolo dell'Osservatorio, 5, I-35122 Padova, Italy; simona.paiano@oapd.inaf.it
[2] INFN, Sezione di Padova, via Marzolo 8, I-35131 Padova, Italy
[3] Università degli Studi dell'Insubria, Via Valleggio 11, I-22100 Como, Italy
[4] INAF, Osservatorio Astronomico di Brera, Via E. Bianchi 46 I-23807 Merate, Italy
[5] Instituto de Astrofisica de Canarias, C/O Via Lactea, s/n, E-38205 La Laguna (Tenerife), Spain
[6] Universidad de La Laguna, Departmento de Astrofísica, s/n, E-38206 La Laguna (Tenerife), Spain
Received 2017 December 22; revised 2018 February 3; accepted 2018 February 5; published 2018 February 23

Abstract

The bright BL Lac object TXS 0506+056 is the most likely counterpart of the IceCube neutrino event EHE 170922A. The lack of this redshift prevents a comprehensive understanding of the modeling of the source. We present high signal-to-noise optical spectroscopy, in the range 4100–9000 Å, obtained at the 10.4 m Gran Telescopio Canarias. The spectrum is characterized by a power-law continuum and is marked by faint interstellar features. In the regions unaffected by these features, we found three very weak (EW ~ 0.1 Å) emission lines that we identify with [O II] 3727 Å, [O III] 5007 Å, and [N II] 6583 Å, yielding the redshift $z = 0.3365 \pm 0.0010$.

Key words: BL Lacertae objects: individual (TXS 0506+056) – galaxies: distances and redshifts – gamma rays: galaxies – neutrinos

1. Introduction

The radio source TXS 0506+056 (3FGL J0509.4+0541) is a bright BL Lac object ($V \sim 15$) that recently became of the utmost astrophysical interest as it is considered to be the probable counterpart of the IceCube neutrino event EHE 170922A of 2017 September 22 (Kopper & Blaufuss 2017). This event is believed to be associated with enhanced γ-ray (100 MeV–300 GeV) activity of the *Fermi*/LAT source 3FGL J0509.4+0541 (Lucarelli et al. 2017; Tanaka et al. 2017) and also with a significant detection at >100 GeV by the Major Atmospheric Gamma Imaging Cherenkov Telescopes (MAGIC; Mirzoyan 2017). An enhanced flux was also revealed in the X-ray regime by the Neil Gehrels *Swift* Observatory (Keivani et al. 2017) and from the All-Sky Automated Survey for Supernovae (ASAS-SN) in the optical band (Franckowiak et al. 2017). During the event, the optical monitoring of the source indicated that the object was ∼0.5 mag brighter in the V band with respect to the previous months.

Optical spectroscopy obtained in previous years by Halpern et al. (2003), Shaw et al. (2013), and Landoni et al. (2013), and after the neutrino event, failed to determine the redshift of this object (Coleiro & Chaty 2017; Morokuma et al. 2017; Soelen et al. 2017; Steele 2017).

Because the knowledge of the TXS 0506+056 distance is necessary to model the spectral energy distribution and the neutrino production mechanism, we undertook a detailed spectroscopic study at the 10.4 m Gran Telescopio Canarias (GTC).

Here we report the results obtained from high signal-to-noise optical observations aimed to pin down the redshift of the source.

2. Observations and Data Analysis

TXS 0506+056 was observed with the GTC at the Roque de Los Muchachos with the spectrograph OSIRIS (Cepa et al. 2003) covering the spectral range 4100–9000 Å. We adopted different grisms (R1000 and R2500) yielding spectral resolution $R = \lambda/\Delta\lambda \sim 600$ and ∼1300. For each setting, we obtained many independent exposures (see Table 1).

Data reduction was carried out using IRAF software and standard procedures for long slit spectroscopy, following the same scheme given in Paiano et al. (2017). The accuracy of the wavelength calibration is 0.1 Å. Relative flux calibration was derived from the observations of spectro-photometric standard stars.

For each data set, we combined the independent exposures, weighting for signal-to-noise ratio (S/N), and anchored the absolute flux to the magnitude of the source ($g = 15.4$), as from acquisition images. Finally, the spectra were dereddened by applying the extinction law of Cardelli et al. (1989), assuming $E_{B-V} = 0.1$ as from the NASA/IPAC Infrared Science Archive 6.[7]

3. Results

In Figure 1 we show the full $R \sim 600$ optical spectrum. The S/N ranges from 650 to 1200 depending on the wavelength. The spectrum is characterized by a non-thermal emission with the power-law shape ($F_\lambda \propto \lambda^\alpha$) with spectral index of $\alpha = -1.0 \pm 0.1$.

Aside from the prominent telluric absorptions and interstellar features, the whole optical spectrum does not exhibit emission or absorption lines with equivalent width (EW) >0.5 Å.

In order to evidentiate the spectral features, we divided the observed spectrum by a fit of the continuum, which was obtained excluding all regions affected by atmospheric and interstellar absorptions (see Figure 2). From the normalized spectrum, we computed the nominal EW in five intervals of the spectra, avoiding the prominent telluric absorption features (see details about the procedure in Appendix A of Paiano et al. 2017). Five different intervals were considered because the S/N depends on the wavelength. This translates into a minimum (3σ level) detectable EW: $\mathrm{EW_{min}} = 0.05$–0.1.

The spectral region between 4100 Å and 4900 Å is affected by diffuse interstellar bands (DIBs; e.g., Herbig 1995) of EW = 0.3–1.0 Å (see Table 2). In addition, the prominent

[7] http://irsa.ipac.caltech.edu/applications/DUST/

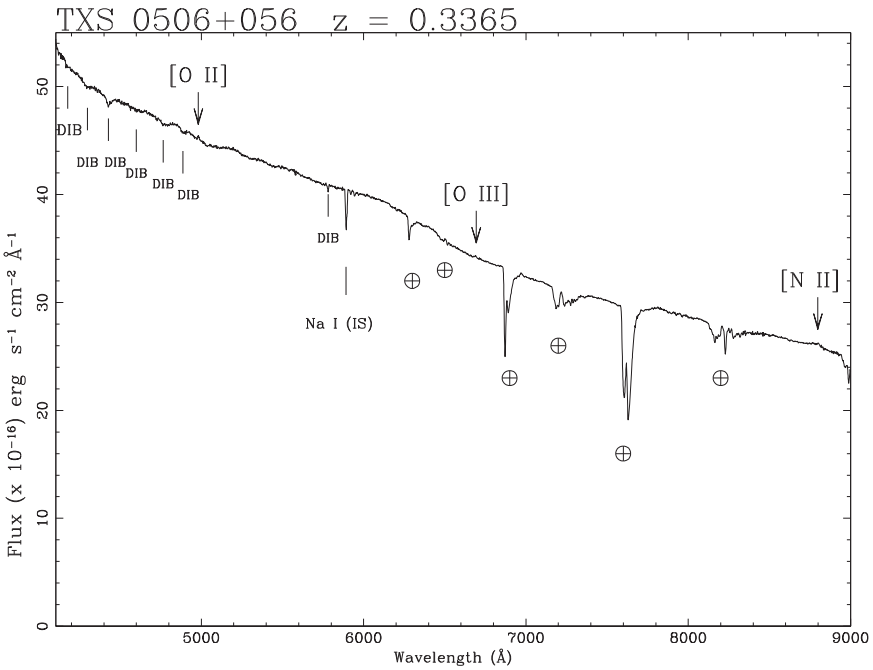

Figure 1. Optical spectrum of the BL Lac object TXS 0506+056 obtained at GTC+OSIRIS ($R \sim 600$). The spectrum is corrected for reddening assuming $E_{B-V} = 0.1$. The shape of the spectrum is dominated by a non-thermal emission and the three arrows indicate the position of the detected emission lines at $z = 0.3365$. Absorption features due to interstellar medium are labeled as DIB and IS. The main telluric bands are marked by $\oplus$.

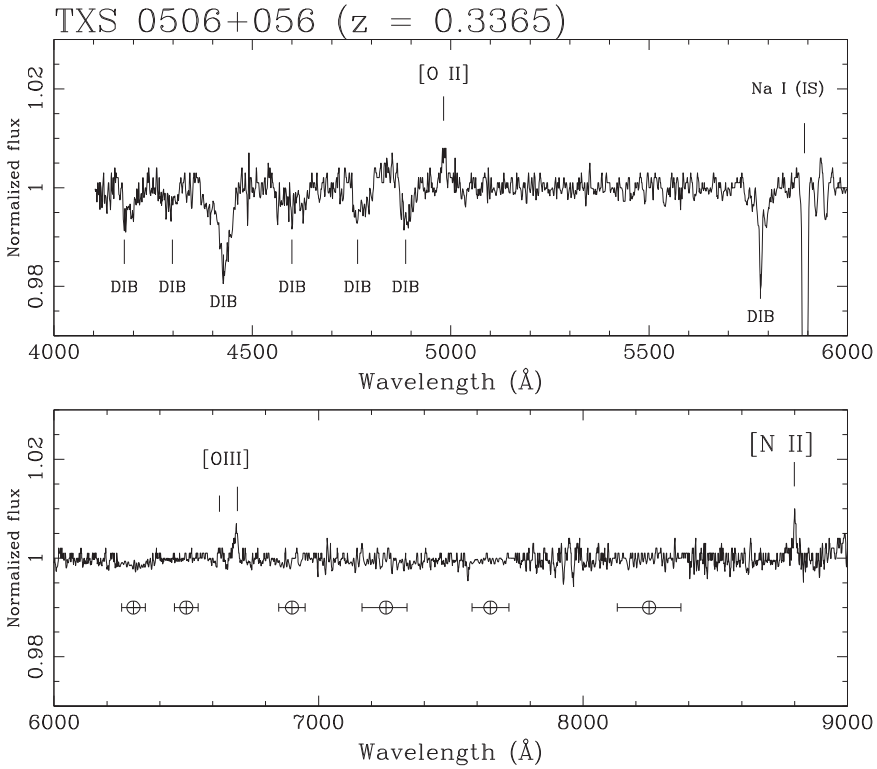

Figure 2. Normalized spectrum of the BL Lac object TXS 0506+056 (see also Figure 1). Three weak (EW ~ 0.1 Å) emission lines are detected and identified as [O II] 3727 Å, [O III] 5007 Å, and [N II] 6583 Å at redshift $z = 0.3365$. Absorption features due to interstellar medium are labeled as DIB and IS. The spectral region affected by telluric absorption, indicated by $\oplus$, were corrected.

(EW = 1.2 Å) interstellar absorption line due to Na I 5892 Å is found.[8]

We search for weak intrinsic absorption and/or emission lines in the spectrum, avoiding all the interstellar spectral features and the regions clearly dominated by the telluric absorptions due to O_2 and H_2O. We detect three faint narrow emission lines at 4981.5 ± 1.0 Å, 6693.6 ± 1.1 Å and at 8800.5 ± 1.1 Å (see Figure 2), identified as [O II] 3727 Å, [O III] 5007 Å, and [N II] 6583 Å, respectively, at $z = 0.336$.

[8] The source is at Galactic latitude $l = -19.^{\circ}6$.

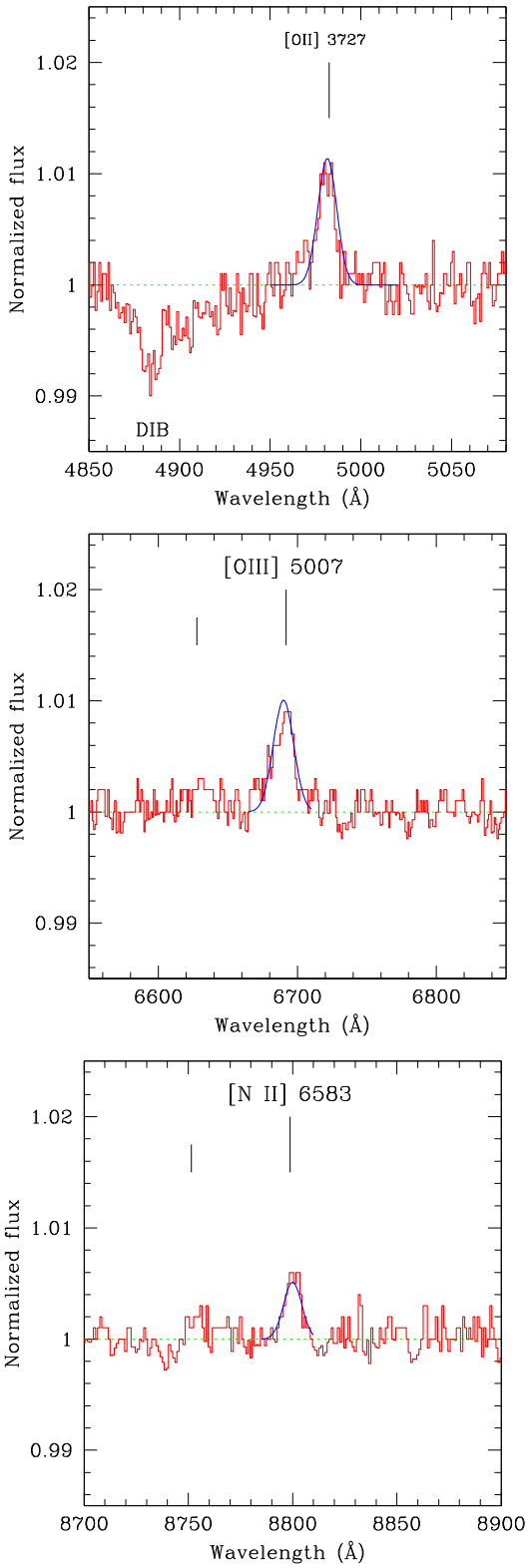

Figure 3. Close-up of the normalized optical spectrum (obtained with $R \sim 1300$) of TXS 0506+056 around the three faint detected emission lines. Top: the emission line at 4981.5 Å identified as [O II] 3727 Å (EW = 0.12 Å). Middle: the emission line at 6693.6 Å identified as [O III] 5007 Å (EW = 0.17 Å), Bottom: the emission line at 8800.5 Å identified as [N II] 6583 Å (EW = 0.05 Å). The short vertical bars indicate the fainter component of the doublet.

The presence of these three emission lines is also confirmed in the observations secured at $R \sim 1300$ resolution (see Table 1). In Figure 3, we reproduce the close-up of the spectral regions around the detected features. For these, we measured EW of 0.12 ± 0.03 Å, 0.17 ± 0.02 Å, and 0.05 ± 0.02 Å), for [O II], [O III], and [N II], respectively.

As a consistency check, we also estimated a redshift lower limit $z > 0.3$, based on the lack of absorption features due to the host galaxy, which is assumed to be a typical giant elliptical of $M(R) = -22.9$ (see for details Paiano et al. 2017).

Table 1
Log of the Observations

Grism	Date	Total Exp. Time (s)	N
R1000B	2017 Nov 23	3600	5
	2017 Dec 05	4200	6
R1000R	2018 Jan 02	4000	6
	2018 Jan 14	4000	6
R2500V	2018 Jan 14	4800	3
	2018 Jan 14	4800	3
R2500R	2018 Jan 15	4500	3
	2018 Jan 20	4800	6
R2500I	2018 Jan 10	4500	3
	2018 Jan 13	4500	2
	2018 Jan 20	4800	6

Note. Column 1: grism name (slit width = 1.0″ for R1000 and slit width = 1.2″ for R2500); Column 2: date of the observation; Column 3: total exposure time; Column 4: number of individual exposures.

Table 2
Optical Spectral Features

λ (Å)	EW (Å)	ID
4190	0.20 ± 0.05	DIB
4290	0.15 ± 0.05	DIB
4427	1.00 ± 0.10	DIB
4600	0.30 ± 0.07	DIB
4770	0.35 ± 0.05	DIB
4890	0.30 ± 0.06	DIB
5780	0.35 ± 0.03	DIB
4981.5	0.12 ± 0.03	[O II] 3727 Å
6693.6	0.17 ± 0.02	[O III] 5007 Å
8800.5	0.05 ± 0.02	[N II] 6583 Å

Note. Column 1: central wavelength of the feature; Column 2: observed equivalent width of the feature; Column 3: feature identification.

4. Conclusions

We obtained an unprecedented high S/N spectrum of the BL Lac object TXS 0506+056, the likely counterpart of the IceCube neutrino event. On the basis of three faint emission lines, we found the redshift is $z = 0.3365 \pm 0.0010$. At this redshift the observed g luminosity is $\nu L_\nu \sim 7 \times 10^{45}$ erg s^{-1}. Assuming that the source is hosted by a typical massive elliptical galaxy (e.g., Falomo et al. 2014), the magnitude is r(host) $\sim$ 18.9. This translates into a total nucleus-to-host ratio >10, which is significantly larger than the average value found for BL Lac objects (see e.g., Scarpa et al. 2000) and is indicative of a highly beamed source. The line luminosities are 2.0×10^{41} erg s^{-1} for the

[O II] and [O III] and 5.0×10^{40} erg s^{-1} for the [N II]. The [O II] luminosity is typical of what is found in quasi-stellar objects (QSOs; see Kalfountzou et al. 2012). The line ratios Log([O II]/[O III]) and Log([N II]/[O II]) are −0.15 and −0.38, respectively. These values are consistent with those typically found for narrow line region emission lines (Richardson et al. 2014). Neither the H_β, that would fall at 6500 Å where a weak telluric absorption is present, nor H_α are detected in our spectra. The optical spectrum of TXS 0506+056 therefore resembles that of a Seyfert 2 galaxy from the point of view of the emission lines. Based on the minimum EW in the regions of these two lines, we estimate that [O III]/$H_\beta \gtrsim 3$ while [N II]/$H_\alpha \gtrsim 2$. These ratios lead to interpret that these emission lines are originated in to the narrow line region of the AGN.

We thank the referee for prompt and constructive criticism and comments.

Facility: GTC-OSIRIS (Cepa et al. 2003).

Software: IRAF (Tody 1986, 1993).

ORCID iDs

Simona Paiano https://orcid.org/0000-0002-2239-3373
Renato Falomo https://orcid.org/0000-0003-4137-6541
Aldo Treves https://orcid.org/0000-0002-0653-6207
Riccardo Scarpa https://orcid.org/0000-0001-9118-8739

References

Cardelli, J. A., Clayton, G. C., & Mathis, J. S. 1989, ApJ, 345, 245
Cepa, J., Aguiar-Gonzalez, M., Bland-Hawthorn, J., et al. 2003, Proc. SPIE, 4841, 1739
Coleiro, A., & Chaty, S. 2017, ATel, 10840, 1
Falomo, R., Pian, E., & Treves, A. 2014, A&ARv, 22, 73
Franckowiak, A., Stanek, K. Z., Kochanek, C. S., et al. 2017, ATel, 10794, 1
Halpern, J. P., Eracleous, M., & Mattox, J. R. 2003, AJ, 125, 572
Herbig, G. H. 1995, ARA&A, 33, 19
Kalfountzou, E., Jarvis, M. J., Bonfield, D. G., & Hardcastle, M. J. 2012, MNRAS, 427, 2401
Keivani, P. A. E. A., Kennea, J. A., Fox, D. B., et al. 2017, ATel, 10792, 1
Kopper, C., & Blaufuss, E. 2017, GCN, 21916, 1
Landoni, M., Falomo, R., Treves, A., et al. 2013, AJ, 145, 114
Lucarelli, F., Piano, G., Pittori, C., et al. 2017, ATel, 10801, 1
Mirzoyan, R. 2017, ATel, 10817, 1
Morokuma, T., Tanaka, Y. T., Ohta, K., et al. 2017, ATel, 10890, 1
Paiano, S., Landoni, M., Falomo, R., Treves, A., & Scarpa, R. , 2017, ApJ, 837, 144
Richardson, C. T., Allen, J. T., Baldwin, J. A., Hewett, P. C., & Ferland, G. J. 2014, MNRAS, 437, 2376
Scarpa, R., Urry, C. M., Falomo, R., Pesce, J. E., & Treves, A. 2000, ApJ, 532, 740
Shaw, M. S., Romani, R. W., Cotter, G., et al. 2013, ApJ, 764, 135
Soelen, B. v., Buckley, D. A. H., & Boettcher, M. 2017, ATel, 10830, 1
Steele, I. A. 2017, ATel, 10799
Tanaka, Y. T., Buson, S., & Kocevski, D. 2017, ATel, 10791
Tody, D. 1986, Proc. SPIE, 627, 733
Tody, D. 1993, in ASP Conf. Ser. 52, Astronomical Data Analysis Software and Systems II, ed. R. J. Hanisch, R. J. V. Brissenden, & J. Barnes (San Francisco, CA: ASP), 173